

Investigation of electrical and magnetical multipoles contributions to the total longitudinal and transverse form factors in some positive and negative ^{27}Al states using different interactions



Nabeel F. Lattoofi, Samaher Th. Mashaan
Department of Physics, College of Science, University of Anbar, Iraq

ARTICLE INFO

Received: 27 / 11 / 2021
Accepted: 16 / 5 / 2022
Available online: 20/7/2022

DOI: 10.37652/juaps.2022.174836

Keywords:

shell model.
electron scattering form factor.
Skyrme interaction.

Copyright©Authors, 2022, College of Sciences, University of Anbar.
This is an open-access article under the CC BY 4.0 license
(<http://creativecommons.org/licenses/by/4.0/>).



ABSTRACT

The shell model and Skyrme interaction calculations were used to study the nuclear structure of the ^{27}Al nucleus. In particular, inelastic electron scattering form factors, energy levels, and transition probabilities for positive and some negative parity low energy states have been calculated. The *sd* shell model was used with *SKX* parameters for positive parity cases. The calculations were performed on *sd* space interactions and the best results were obtained from *HBUMSD*, *HBUSD*, *CWH*, *PW*, and *W* interactions. For negative parity cases, the *z_{bm}* model space with *SKX_{csb}* parameters has been used with *z_{wm}* interactions. The excitation energies and transitions probabilities to the ground state $5/2^+$ for positive parity states have been also calculated. The calculated form factors, energy level diagrams, and transition probabilities were compared with the available experimental data. It was confirmed that the Skyrme interaction is suitable with the shell model to study the nuclear structure.

1. Introduction

Nuclear and Particle physics are one of the most important fundamental physics fields quest to study the structure of atomic nuclei. The most championed scientific tool used for this purpose is the electron scattering which gives important information about the inner structure of nuclei. The weak well understood electromagnetic force of electrons interacting with the nucleus gives electrons the greatest advantage as a probe. As a result, nuclear characteristics may be retrieved unambiguously from the data, as unknown probe properties are excluded from the analysis. Elastic electron scattering gives structure information about the nucleus in its ground state. When energy transferred to the nucleus increase, the interaction starts to become more inelastic and can be used to stimulate the nucleus to a higher excited state, which is often described in the context of the nuclear shell model description of a discrete nucleon excitation.

The low-lying odd and even parity states for the very interesting *sd* shell nuclei have received attention recently from both experimental and theoretical points of view.

These nuclei have been used for studying the applicability of nuclear models such as the nuclear shell model which is one of the most successful models in describing the nuclear structure. In this study, we present the ^{27}Al nucleus as a single-*A* light nucleus that lies in the transitional region where the nuclear deformation changes from prelate for ^{26}Mg to oblate for ^{28}Si .

The features, both static and dynamic, of this nuclear system, have been studied in a number of research. For the ground states with $J = 3/2^+$ and $J = 5/2^+$, shell wave functions for $A = 19-39$ cores were utilized to construct the one-body densities on which the M1, E2, M3, E4, and M5 moments are based. authored by B. Brown, A. *et al.*, [1] Theoretical values were compared to experimental data and assessed in terms of deviations from the predictions of the pure formation envelope model. The even-parity states of ^{27}Al below 7 MeV, inelastic electron scattering form factors were observed By P. J. Ryan *et al.*, [2] the data span a momentum transfer range of ($q=0.75$ to 2.80 fm^{-1}). Brown, B., *et al.*, [3] study electron scattering on ^{19}F is described in its entirety, both theoretically and experimentally. Theoretical approaches for deriving the various components of electron scattering form factors from multiparticle shell-model wave functions are outlined. They employed *1s0d* shell-model wave functions generated with a new "universal" Hamiltonian, and *0p-1s0d* shell-model wave

*Corresponding author at: Department of Biology , Collage of Science , University Of Anbar , Anbar , Iraq
dr.nabeel.fawzi@uoanbar.edu.iq

functions based on Millener and Kurath's cross-shell Hamiltonian for negative-parity states. For momentum transfers up to 2.4 fm^{-1} , the comparisons are done with measured longitudinal and transverse form factors.

Electron scattering form factors for the low positive valences of ^{27}Al were performed by R.A. Radhi [4]. Strong excitation of M1 and M3 was observed by magnetic form factors for the low states at ^{27}Al by R.A. Radhi *et al.* [5] who studied the magnetic formations of the elastic core of the ground state $5/2^+$ within $0.5 - 2.5 \text{ fm}^{-1}$ transfer momentum region.

Predictions for a large area The longitudinal and transverse (electrical) form factors from the excitation of 2^+_1 and 4^+_1 instances at ^{12}C , ^{20}N , and ^{24}Mg were calculated using Hartree-Fock wave functions. The results of such large-structure-based space models are contrasted to finite-base-space predictions (the shell model) to demonstrate that momentum-transfer-dependent corrections can be quite varied. authored by Amos, K. and C. Steward [6].

Elastic and inelastic electron scattering agents for light nucleus, including ^{27}Al , were studied by Khalid S. Jassim *et al.* [7] for the momentum transfer region 0.5 and 2.5 fm^{-1} .

Ali A. Alzubadi *et al* studied the inelastic electronic form factors for the positive and negative parity states of the ^{19}F nucleus [8] within $0.6 - 2.5 \text{ fm}^{-1}$ transfer momentum region. Hartree-Fock's field approach with Skyrme type interaction has been stressed as the best and most suited method for the shell model. Longitudinal and transverse electron form factors of the ^{17}O nucleus were studied for positive and negative parity states by Ali A. Alzubadi *et al* [9]. Shell model and self-consistent Hartree-Fock computations were used for analyzing ^{17}O nuclear structures. For this objective, two alternative shell model spaces were used. The first is the *psd_{pn}* model space for positive parity states, while *zmb_e* has been presented for states with negative parity.

This study is concerned in investigating the total electrical and magnetical contributions to the longitudinal, transverse inelastic form factors in some positive and negative ^{27}Al parity states. The *sd* model with SKX parameters was used with positive parity states consisting of the active $1d_{5/2}$, $2s_{1/2}$ and $1d_{3/2}$ shells above the inactive ^{16}O core in $(1s)^4(1p)^{12}$ which remains closed. The interactions HBUMSD, HBUSD, CWH PW and *W* were used to provide realistic sd-shell wave functions ($1d_{5/2}$, $1d_{3/2}$, $2s_{1/2}$) for positive valence states $5/2^+$ ground state (GS) $5/2^+$, $1/2^+$ (0.844 MeV), $3/2^+$ (1.014 MeV), $5/2^+$ (2.735 MeV), $7/2^+$ (2.211 MeV) and $9/2^+$ (3.004 MeV). The *zmb* model space with SKXcsb parameters was used for the $1/2^-$ (4.055 MeV), $3/2^-$ (5.156 MeV) and $3/2^-$ (5.827 MeV) negative parity states.

The matrix element of single-particle for all excited states was derived using Skyrme interaction with various

parameterizations. The Skyrme interaction generates an analytic energy density functional that can be swiftly computed to yield minimal energy and single-particle densities. This model has shown to be very useful for nuclear mean-field (MF) computations since Vautherin and Brink [10] implemented the Skyrme interaction. It allows for the truncation of the shell-model space to a closed-shell configuration as well as three-body interactions with a minimal set of parameters, such as expansions of *s* and *p*-wave of an effective nucleon–nucleon interaction, as well as the dependent density part. The interaction parameters must be determined from experimental data because it is phenomenological [11].

2. Theory and methodology

The total form factor can be represented with the electron scattering angle θ as the sum of the two terms; longitudinal $F^L(q)$ and transverse $F^T(q)$ as follows:

$$|F(q)|^2 = |F^L(q)|^2 + [1/2 + \tan^2(\theta/2)][F^T(q)]^2 \quad (1)$$

For the total form factors, longitudinal (*L*) and transverse (*T*), it can be written as [12]:

$$|F^L(q)|^2 = \sum_{J \geq 0} |F^L_J(q)|^2 \quad (2)$$

$$|F^T(q)|^2 = \sum_{J \geq 0} \left\{ |F^M_J(q)|^2 + |F^E_J(q)|^2 \right\} \quad (3)$$

where $|F^E_J(q)|^2$ and $|F^M_J(q)|^2$ are the transverse electric and magnetic form factors, respectively.

The sum of the product of the elements of the one-body density matrix (OBDM) $X^J_{j_f j_i}(t_z, j_i, j_f)$ and the single-particle matrix elements represented the reduced matrix element of the electron scattering operator \hat{T}_{J,t_z} for a chosen model space and is given by [12]:

$$\langle J_f || \hat{T}_{J,t_z} || J_i \rangle = \sum_{j, j_f} X^J_{j_f j_i}(t_z, j_i, j_f) \langle J_f || \hat{T}_{J,t_z} || J_i \rangle \quad (4)$$

with initial and final single-particle states with in concerning model space j_f and j_i and $t_z = 1/2$ and $-1/2$ for proton and neutron respectively.

Center of mass $F_{cm}(q)$ and finite-size $F_{fs}(q)$ corrections were included the electron scattering form factor involving momentum transfer q , between initial and final states of spin $J_{i,f}$ as follows [13]:

$$|F^{\eta}(q)|^2 = \frac{4\pi}{Z^2(2J_i + 1)} \left| \sum_{t_z} e(t_z) \langle J_f || \hat{T}_{J,t_z}^{\eta}(q) || J_i \rangle \right|^2 F_{cm}^2(q) F_{fs}^2(q) \quad (5)$$

with η is either the longitudinal (L) or transverse (T) form factors.

The reduced transition probability is given by [3]

$$B(\eta J) = \frac{Z^2}{4\pi} \left[\frac{(2J+1)!!}{k^J} \right]^2 [F_J^\eta(k)]^2 \quad (6)$$

where $k=E_x/\hbar c$.

$$B(\eta J)J_i = \frac{1^+}{2} \rightarrow J_f, B(M1) \text{ in units of } u_N^2, B(E2) \text{ in units of } u_N^2 \text{ fm}^2, B(E1) \text{ units of } e^2 \text{ fm}^2$$

The central potential is represented here with the one-body mean-field Skyrme potential were used for which is an approximated field provided from all two and three body interactions between nucleons inside the nucleus. This potential can be given in terms of two-and three-body parts as follows [10]:

$$\hat{V}_{Skyrme} = \sum_{i<j} V_{ij}^{(2)} + \sum_{i<j<k} V_{ijk}^{(3)} \quad (7)$$

The two-body part is given by

$$\begin{aligned} \hat{V}^{(2)}_{Skyrme} &= \hat{V}^m + \hat{V}^{LS} + \hat{V}^t \\ \hat{V}^m &= t_0(1 + x_0 \hat{p}_\sigma) \delta_{12} + \frac{t_3}{6} (1 + x_3 \hat{p}_\sigma) \rho^\alpha(r_1) \delta_{12} + \frac{t_1}{2} (1 + x_1 \hat{p}_\sigma) (\delta_{12} \hat{k}^2 + \widehat{K} \delta_{12}) + (1 + x_2 \hat{p}_\sigma) \hat{k}' \hat{k} \delta_{12} \\ \hat{V}^{LS} &= it(\hat{\sigma}_1 + \hat{\sigma}_2) \cdot \hat{k}' * \hat{k} \delta_{12} \\ \hat{V}^t &= \frac{t_e}{2} \left\{ (3(\hat{\sigma}_1 \hat{k}')(\hat{\sigma}_2 \hat{k}') - (\hat{\sigma}_1 \hat{\sigma}_2) \hat{k}'^2) \delta_{12} + \delta_{12} (3(\hat{\sigma}_1 \hat{k})(\hat{\sigma}_2 \hat{k}') - (\hat{\sigma}_1 \hat{\sigma}_2) \hat{k}^2) \right\} + t_0 (3(\hat{\sigma}_1 \hat{k}') \delta_{12} (\hat{\sigma}_2 \hat{k}') - (\hat{\sigma}_1 \hat{\sigma}_2) \hat{k}' \cdot \delta_{12} \hat{k}) \end{aligned} \quad (8)$$

were $\delta_{12} = \delta(r_1 - r_2)$ and the three-body part by

$$V_{Skyrme}^{(3)} = t_3 \delta_{12} \delta_{13} \quad (9)$$

The \hat{k} and \hat{k}' are relative momentum operators which are defined as

$$\hat{k} = \frac{1}{2i} (\vec{\nabla}_1 - \vec{\nabla}_2), \quad \hat{k}' = \frac{1}{2i} (\overleftarrow{\nabla}_1 - \overleftarrow{\nabla}_2) \quad (10)$$

with the \hat{k}' acting to the left. The tensor force is usually neglected.

The saturation properties have been presented in the first item of Equ.(8), while surface properties were shown in momentum-dependent terms which is account for finite-range force effect [14]. SkXcsb parameterizations were implemented in this study [15] which delivers the best rms (root-mean-square) results. Direct and exchange Coulomb (CD and CE) factors as well as the Charge

symmetry breaking (CSB) in the s wave section, are included in this parameterization. Folding the computed charge distribution, $P_{ch}(r)$, with the two-body Coulomb interaction yields the direct Coulomb potential, which is given by [16].

$$H_{CD} = \frac{e^2}{2} \iint_{00}^{\infty \infty} \frac{\rho_P(r) \rho_P(r')}{|r - r'|} d^3r d^3r' \quad (6)$$

The Coulomb interaction exchange part comes from the Slater approximation and as a function of density matrix expansion:

$$H_{CE} = \frac{3e^2}{4} \left(\frac{3}{\pi}\right)^{1/3} \int_0^\infty \rho_P(r)^{4/3} d^3r \quad (7)$$

3. Results and Discussion

The latest version of the OXBASH shell model code uses proton and neutron formalisms have been obtained to calculate the OBDM elements which used then in MJ and EJ matrix elements operators. The single particle elements of radial wave functions were computed using the SHF potentials of the type SkX and SkXcsb types for conditions of positive and negative parity, respectively. Results will be separated into two parts for discussion. The first part included the positive parity states form factors, transition probabilities and energy levels. The inelastic form factors for the negative parity states were included in the second part.

3.1. States with a positive parity

The calculations of longitudinal and transverse form factors in positive low parity states case have been adopted using distinct two-body effective interactions utilizing the sd -model space. Fig. 1(a) shows the total inelastic longitudinal form factors (C0+C2+C4) for the first $5/2^+$ at energy 2.734 MeV calculated with sd model space using SKX parameterizations for all interactions identified. This figure shows that all interactions are suitable for reproducing experimental form factors data in the area where momentum is transferred between (0.5 to 2.4 fm^{-1}). The shape of the theoretical curve agrees well with the Experimental for all interactions. In terms of longitudinal form factors, Contributions were made of the coulomb C0,C2,C4 form factors for the best HBUMSD interaction concluded from Fig.1(a) were illustrated in Fig.1(b). We notice a small contribution of C0 which is considered negligible. The contribution of C2 with the experimental data has been noticed to be considered in the momentum transfer region (0.5 to 1 fm^{-1}) and C4 is the most contributory in the region above 1.5 fm^{-1} .

The total transverse form factors (electrical and magnetic), Fig.1(a and b), were shown in Fig.1(c) for all interactions. The two peaks, at the 1 and 2.25 fm^{-1} , have been represented very well by theoretical curves. It agrees with the results of the experiment for all interactions in the

transfer of momentum region (0.75 to 3 fm⁻¹). Fig.1(d) represents the contribution of the total magnetic M1+M3 and total electric E2+E4 form factors using the HBUMSD interaction. One notices that the main contribution belongs to the total magnetic form factors M1+M3 which show the largest contribution in the transfer of momentum region (0.75 to 3 fm⁻¹).

Fig.2(a) shows the inelastic longitudinal C2 form factor for the first 1/2⁺ (0.844 MeV) state using also the five interactions chosen with SKX parameters give a fine agreement with the momentum transfer experimental data region (0.6 to 2.5fm⁻¹). The calculated curves represented by two peaks are overestimating the experimental data for the region (0.5 to 1.5 fm⁻¹). For the second peak one can see that the calculated results are underestimating the experimental data. The inelastic (electrical and magnetic) transverse form factors are shown in Fig.2(b). The calculated results show better agreement with experimental data for the second peak with transfer of momentum over 1.5 fm⁻¹, than the first peak in which our results higher than the experimental one. Fig.1(c) shows the contribution of the electric (E2) and magnetic (M3) the proportion of transverse form factors in the total transvers form factor calculated using HBUMSD interaction along with the experimental data. It was observed that the main contribution is given by M3 at the higher momentum transfer region larger than (1.5 fm⁻¹), while the contribution of E2 appears greater for low momentum transfer regions (smaller than 1.5 fm⁻¹). In general, the results represented the whole transvers shape very well.

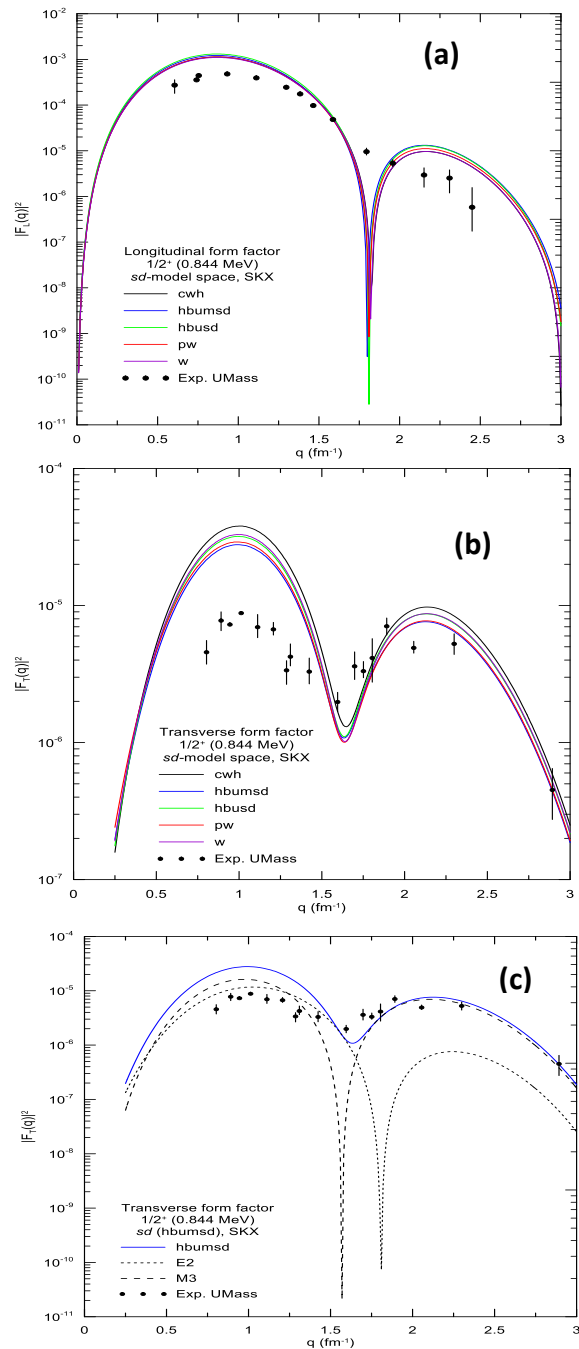


Fig.2: Calculated longitudinal (a) and transverse (b and c) form factors for (0.844 MeV 1/2⁺) compared to experimental data using SkX parameterization [2].

The computed C2+C4 longitudinal form factors were calculated for first 3/2⁺ state at 1.014 MeV. An examination of these curves in Fig.3(a) reveals that the predictions using SKX parameters are in good agreement with the results of the experiments. The longitudinal form factors were calculated for this transition, where the total sum of the C2+C4 longitudinal shape factors agrees well with the experimental data for the five interactions selected for the a range of momentum transfer regions from (0.6 to 2.5 fm⁻¹). In Fig. 3(b) one can notice clearly that the main contribution to the total longitudinal form factors belongs to C2 curve for all momentum transfer, while C4 contribution is considered negligible. Fig.3(c) represents the transverse

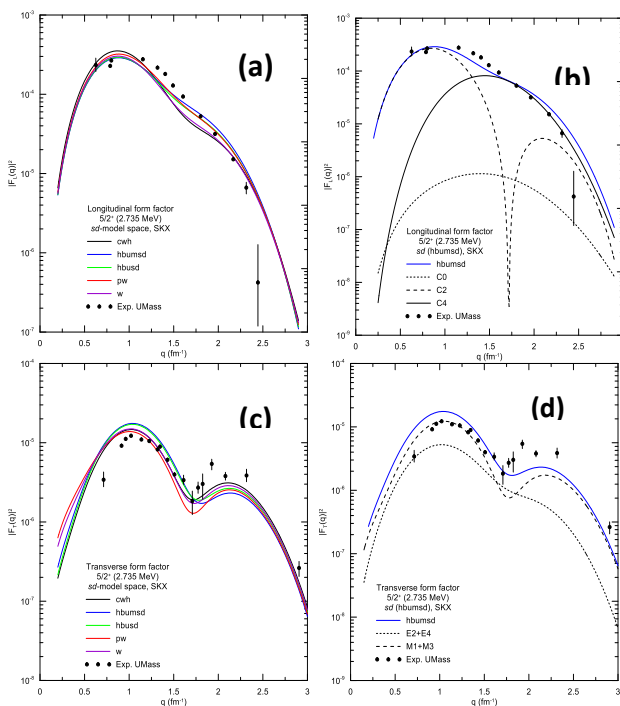


Fig.1: Calculated longitudinal (a and b) and transverse (c and d) form factors for (2.735 MeV 5/2⁺) compared to experimental data using SkX parameterization [2].

form factors of the sum of E2+E4 and M1+M3 for the five selected reactions. The agreement is good with the results of the experiment for the second peak with transfer of momentum larger than 1.75 fm^{-1} . For the region of momentum transfer (0.75 to 1.75 fm^{-1}) the experimental data are underestimate the theoretical curves. Fig.3(d) represents the contributions of the total electric and magnetic form factors with the best interaction (HBUMSD).

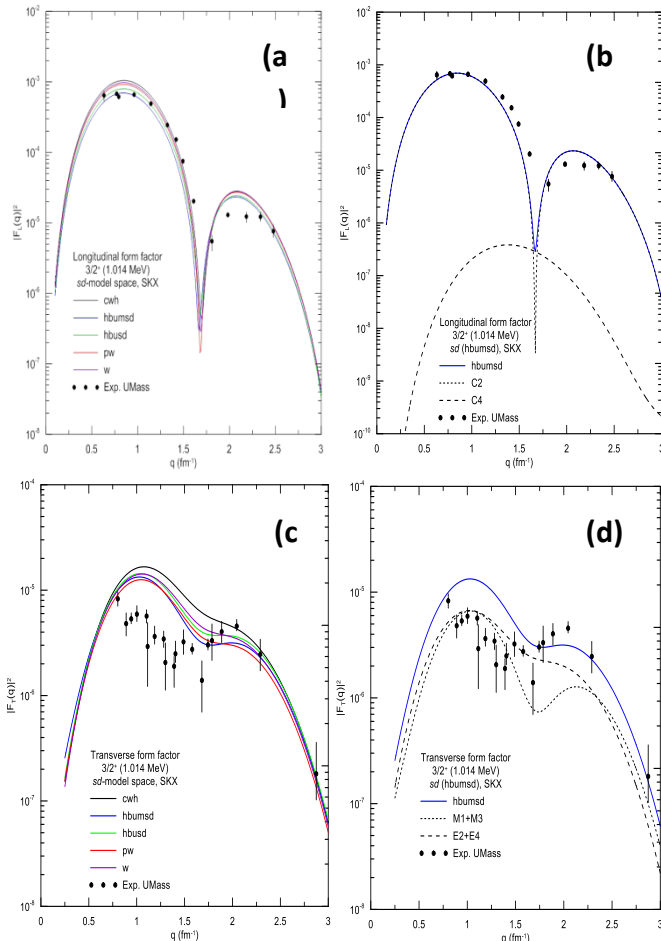


Fig.3: Calculated longitudinal (a,b) and transverse (c,d) form factors for (1.014 MeV $3/2^+$) compared to experimental data using SkX parameterization [2].

Fig.4(a) shows C2+C4 inelastic longitudinal form factors for the transition $7/2^+$ (2.211 MeV) for all interactions selected in the momentum transfer region (0.3 to 2.5 fm^{-1}) along with experimental data. The calculated results are in complete agreement with experimental findings one for all interactions. Fig.4(b) represents the best interaction of CWH with the contribution of both C2 and C4 with the experimental data. The contribution of C4 was almost negligible, while the contribution of C2 is greater and can be considered for all momentum transfer region. Fig.4(c) shows the overall transverse form factors that correspond well in the momentum regions. (0.4 to 3 fm^{-1}) to the experimental curve is located on top of the theoretical curve. Fig.4(d) represents the best interaction with the contributions of transverse form factors (electrical and magnetic), as it was noticed that electric (E2+E4) curve

gives a good contributes to the total transverse form factor in the low and medium momentum transfer, and the largest contribution is clearly belongs to the magnetic (M1+M3+M5) curve.

In Fig. (5.a) the calculated inelastic longitudinal form factors C2 + C4 for the transition $9/2^+$ at (3.004 MeV). Our results are in complete agreement with experimental findings in momentum region (0.3 to 2.5 fm^{-1}) of all the five selected interactions especially with HBUMSD interaction. The individual C2 and C4 contributions to the longitudinal form factor have been shown in Fig.5(b) along with the results of the experiment for the best interaction. The contribution of C4 is observed to be considered for over 1.5 fm^{-1} , while the contribution of C2 is significantly for the transmission of all momentum. The transverse form factors of this transition represented by the sum of the magnetic and electrical form factors for each selected interaction were dissipated in Fig.5(c). All interactions are in excellent agreement with the results of the experiments at the momentum transfer region (0.4 to 2.9 fm^{-1}).

Fig.5(d) shows the best interaction with the contribution of the electric curve E2+E4 and the magnetic M3+M5 curves. We notice that the contribution of E2+E4 is large, while the contribution of M3+M5 is considered for high transfer of momentum (over 1.5 fm^{-1}).

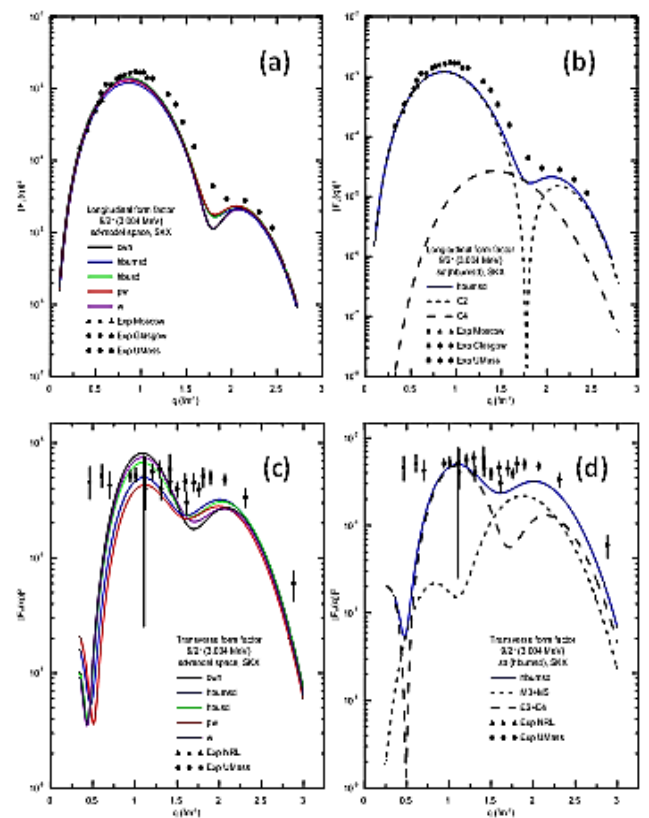


Fig. 4: Calculated Longitudinal (a,b) and transverse (c,d) Form factors for (2.211 MeV $7/2^+$) compared to experimental data using SkX parameterization [17, 18].

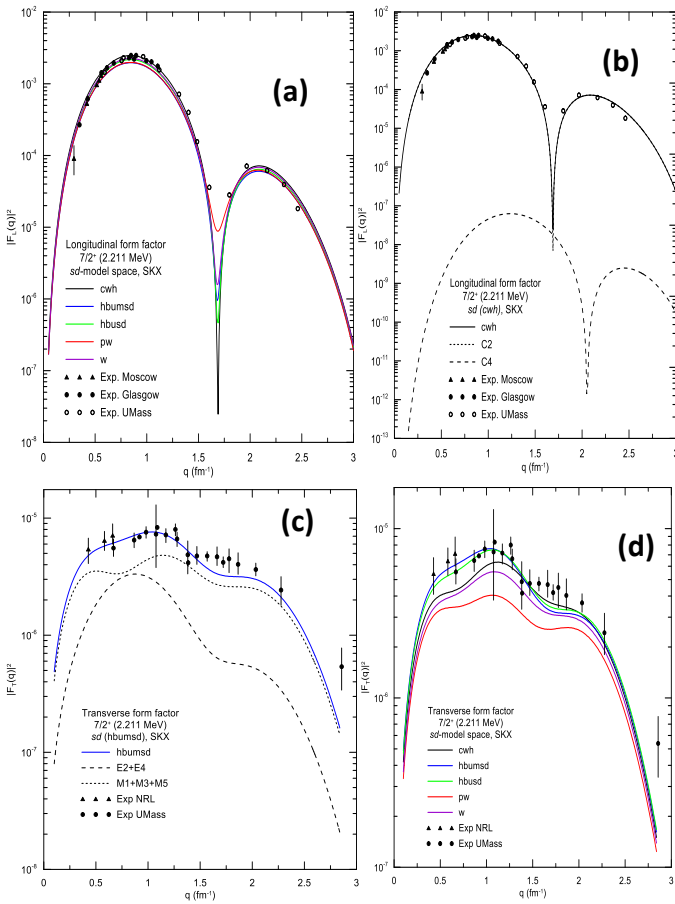


Fig.5: Calculated Longitudinal (a,b) and transverse (c,d) form factors for (3.004 MeV 9/2+) compared to experimental data using SkX parameterization [2].

Fig. 6(a) represents the inelastic form factors of the $11/2^+$ transition at 4.580 MeV for all interactions. it was found that the theoretical curves are in excellent agreement with the experimental data. The most compatible interactions for this transition are HBUMSD, CWH and W, within the transmission of momentum region (0.75 to 2.5 fm⁻¹). Fig. 6(b) represent all the obtained multipoles (longitudinal and transverse) (C4, E4, M3, M5) for this inelastic transition. The figure clearly appear the dominate and strong contributions of the longitudinal C4 multipole, while the contribution of E4,M3,M5 are small and negligible.

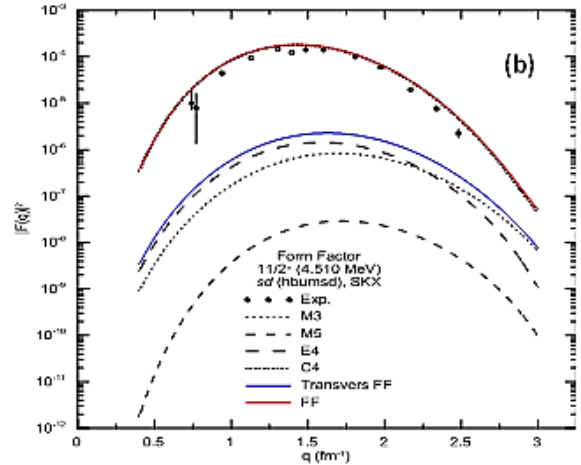
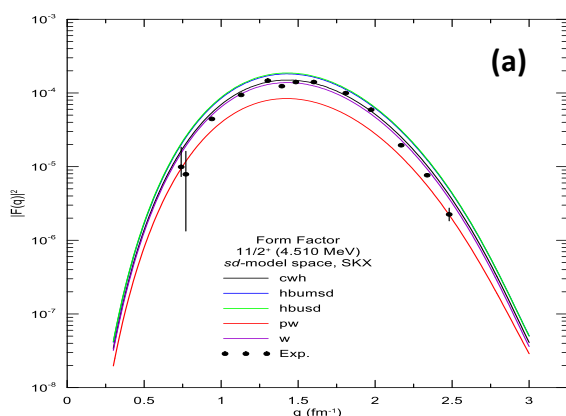


Fig.6: Total form factors for (4.580 MeV 11/2⁺) compared to experimental data using SkX parameterization [2].

Fig.7 show a comparison between the calculated energy levels with the experimental energy spectrum for different interactions selected in this study. although the agreement between the theoretical and experimental schemes has not been implemented with great success, one can conclude that the reaction W is the most consistent reaction with the practical results, followed by the HBUSD reaction.

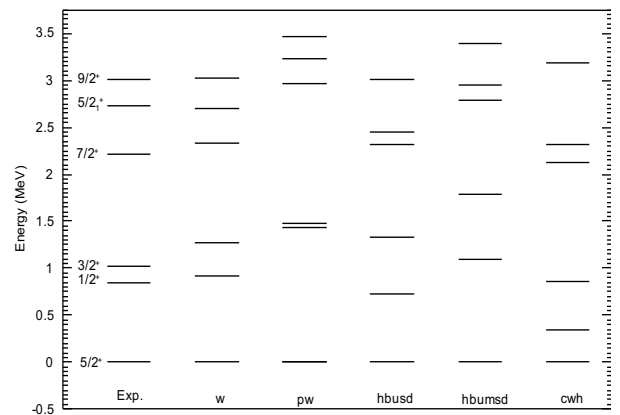


Fig. 7: Comparison of positive parity energy levels of the ^{27}Al nucleus using different interactions.

Table1: Reduced transition probabilities and excitation energies for ^{27}Al nucleus (states with a positive parity)

$J_i^\pi \rightarrow J_f^\pi$	Excitation energy (MeV)		B(E2)(e ² fm ²)	
	Theory	Exp.	Theory	Exp.
$5/2^+ \rightarrow 1/2^+$	0.921	0.844	46.4	12.7±0.5
$5/2^+ \rightarrow 3/2^+$	1.294	1.014	28.89	25.5±2.6
$5/2^+ \rightarrow 7/2^+$	2.326	2.212	82.19	94.6±5.4
$5/2^+ \rightarrow 5/2^+$	2.704	2.734	11.27	8±3
$5/2^+ \rightarrow 9/2^+$	3.026	3.004	46.6	55.9±3.2
$5/2^+ \rightarrow 11/2^+$	4.580			

3.2. Negative parity states

The *zbm* model space has been used with SkXcsb parameters for the calculations of the negative parity states. The *zwm* two body interactions are the only interactions which used for these calculations. The longitudinal and transverses for the initial excitation $1/2^{-1}$ state at 0.055 MeV have been calculated and shown in Fig.8 (a and b), as well as the experimental points. The pure longitudinal C3 and transverse E2,M3 are present in this transition. The shape of the computed form factors calculated with SkXcsb parameterization is in qualitative agreement with the experimental one, according to these curves in the transfer of momentum region (0.75 to 2.5 fm^{-1}). The results showed that the shape of the theoretical curve is the same as the shape of the experimental curve represented by one peak. Fig. 8(b) represents the transverse form factors (E3,M2) and their sum. The results are not in good agreement with the results of the experiments. As one can see from the figure that our results are overestimate the experimental one. In comparison to actual data, the shape of the computed E3+M2 form factor is well reproduced, however in low momentum transfer region it is underestimated. The two figures show that the longitudinal form factors correspond well and better than the transverse form factor.

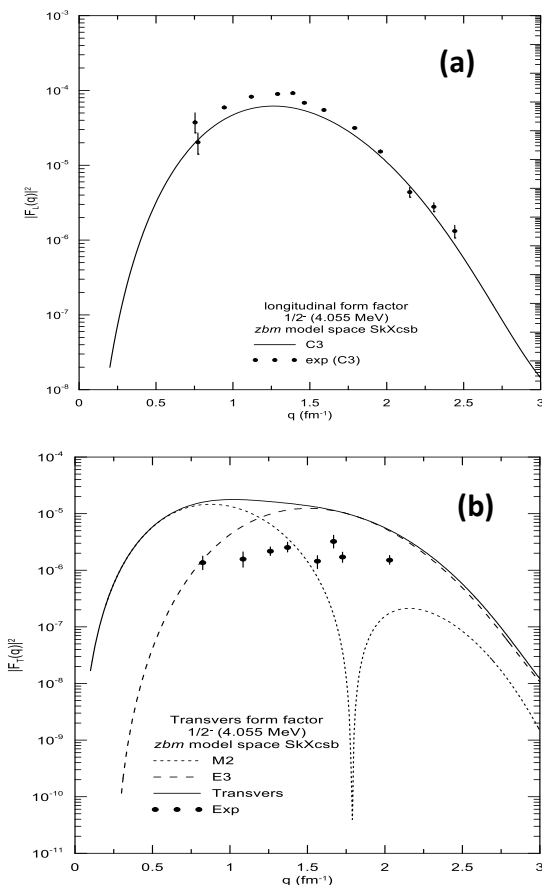


Fig 8. Theoretical longitudinal (a) and transverse (b) form factors for the negative parity state $1/2^{-1}$, 0.055MeV using *zbm* with SkXcsb parameterization compared with experimental data[19]

The calculated longitudinal form factors for the first and second negative-parity state $3/2_1^{-}$ (5.156 MeV) and $3/2_2^{-}$ (5.827 MeV) were shown in Fig. 9 (a and b) respectively with the experimental one. The total longitudinal form factors for transition $3/2_1^{-}$ represented by (C1+C3) agrees well with the experimental data especially when the momentum transfer is higher than (1.5 fm^{-1}) and the contribution of C1 is lower than C3.

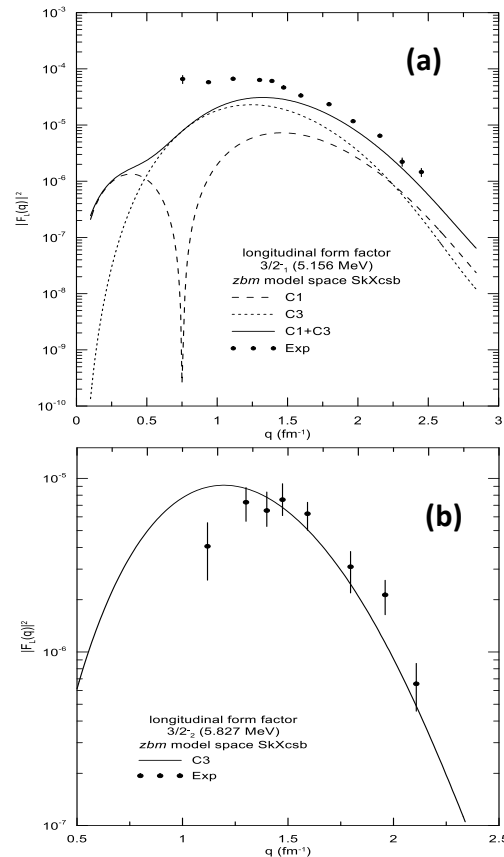


Fig.9. Theoretical longitudinal form factors for the first negative parity state $3/2_1^{-}$, 5.156 MeV (a) and (b) second negative parity state $3/2_2^{-}$, 5.827 MeV using *zbm* with SkXcsb parameterization compared with experimental data [19].

For the $3/2_2^{-}$, (5.827) MeV state, the shapes of the form factors are in qualitative agreement with these data. Little discrepancy can be noticed in longitudinal form factor the calculated C3 at medium momentum transfer. The calculated results are in general in a good agreement with the experimental data.

4. Conclusions

It has been emphasized that the Skyrme interaction is probably the best and most appropriate interaction with the shell model in calculating single-section array elements to study nuclear structure and is necessary to obtain a reasonable description of the longitudinal and transverse electron scattering form factor. For energy level and transition probabilities, it has been found the best interaction for *sd*-model space the experimental data is *W* interaction followed by *HBUM*. For negative parity states model space,

the interaction used can not represent the experimental data for all states. It has been shown that the main contribution to the longitudinal form factors belongs to the (C2) Coulomb multipoles. For the transvers form factors it's clearly shown that contributions of total magnetic form factors are dominant and larger than total electric ones.

5. References

- [1] B. Brown, W. Chung, B. Wildenthal, Electromagnetic multipole moments of ground states of stable odd-mass nuclei in the sd shell, *Physical Review C*, 22 (1980) 774.
- [2] P. Ryan, R. Hicks, A. Hotta, J. Dubach, G. Peterson, D. Webb, Electroexcitation of even-parity states in Al 27, *Physical Review C*, 27 (1983) 2515.
- [3] B. Brown, B. Wildenthal, C. Williamson, F. Rad, S. Kowalski, H. Crannell, J. O'Brien, Shell-model analysis of high-resolution data for elastic and inelastic electron scattering on F 19, *Physical Review C*, 32 (1985) 1127.
- [4] R. Radhi, Nuclear structure study with inelastic electron scattering from 27Al, *Nuclear physics A*, 707 (2002) 56-64.
- [5] R. Radhi, N. Khalaf, A. Najim, Elastic magnetic electron scattering from 17O, 25Mg and 27Al, *Nuclear Physics A*, 724 (2003) 333-344.
- [6] K. Amos, C. Steward, Large basis space effects in electron scattering form factors of light nuclei, *Physical Review C*, 41 (1990) 335.
- [7] K.S. Jassim, A.A. Al-Sammarrae, F.I. Sharrad, H.A. Kassim, Elastic and inelastic electron-nucleus scattering form factors of some light nuclei: Na 23, Mg 25, Al 27, and Ca 41, *Physical Review C*, 89 (2014) 014304.
- [8] R. Radhi, A.A. Alzubadi, E.M. Rashed, Shell model calculations of inelastic electron scattering for positive and negative parity states in 19F, *Nuclear Physics A*, 947 (2016) 12-25.
- [9] A.A. Alzubadi, R. Radhi, N.S. Manie, Shell model and Hartree-Fock calculations of longitudinal and transverse electroexcitation of positive and negative parity states in O 17, *Physical Review C*, 97 (2018) 024316.
- [10] D. Vautherin, D.t. Brink, Hartree-Fock calculations with Skyrme's interaction. I. Spherical nuclei, *Physical Review C*, 5 (1972) 626.
- [11] B.A. Brown, Synthesis of mean-field and shell-model configuration-mixing methods, *Riken Review*, DOI (2000) 53-57.
- [12] P.B.a.P. Glaudemans, *Shell-Model Applications in Nuclear Spectroscopy*, North-Holland, Amsterdam and New York 1979.
- [13] T. de Forest Jr, J.D. Walecka, Electron scattering and nuclear structure, *Advances in Physics*, 15 (1966) 1-109.
- [14] H. Sagawa, B. Brown, O. Scholten, Shell-model calculations with a Skyrme-type effective interaction, *Physics Letters B*, 159 (1985) 228-232.
- [15] B. Brown, W. Richter, R. Lindsay, Displacement energies with the Skyrme Hartree-Fock method, *Physics Letters B*, 483 (2000) 49-54.
- [16] J. Negele, D. Vautherin, Density-matrix expansion for an effective nuclear hamiltonian, *Physical Review C*, 5 (1972) 1472.
- [17] R.P. Singhal, A. Johnston, W.A. Gillespie, E.W. Lees, Inelastic scattering of electrons from 27Al, *Nuclear Physics A*, 279 (1977) 29-44.
- [18] J.W. Maas, A.J.C.D. Holvast, A. Baghus, H.J.M. Aarts, P.M. Endt, Bound states of 27Al studied at selected 26Mg(p, γ)27Al resonances, *Nuclear Physics A*, 301 (1978) 237-257.
- [19] R.S. Hicks, A. Hotta, J.B. Flanz, H. deVries, Electroexcitation of odd-parity states in 27Al, *Physical Review C*, 21 (1980) 2177-2189.

دراسة مساهمة الاقطاب الكهربائية والمغناطيسية لعوامل التشكل الكلية الطولية والمستعرضة لبعض مستويات الالمنيوم-27 الموجبة والسالبة باستخدام تفاعلات مختلفة.

نبيل فوزي لطوفي ، سماهر ثابت مشعان
جامعة الانبار - كلية العلوم - قسم الفيزياء

الخلاصة:

استخدمت حسابات نموذج القشرة وتفاعلات سكيرم لدراسة التركيب النووي لنواة الالمنيوم-27. بشكل عام تم حساب عوامل التشكل للاستقطاب الإلكتروني الغير مرنة، مستويات الطاقة وعوامل الانتقال لمستويات الطاقة الواطنة ذوات التماثل الموجب والسالب. استخدم فضاء نموذج القشرة sd مع معلمات SKX لحالات التماثل الموجب. جهزت الحسابات لتفاعلات فضاء sd وافضل النتائج هي المعتمدة من التفاعلات HBUMSD, HBUSD, CWH, PW و. لحالات التماثل السالب، تم استخدام موديل فضاء zbm مع معلمات SKXcb وباستخدام تفاعل zwm مستويات طاقات التهيج واحتمالات الانتقال الى المستوى +2/5 الارضي تم حسابها ايضا. تم مقارنة نتائج عوامل التشكل ومستويات الطاقة واحتمالات الانتقال مع البيانات العملية. تم التأكيد على ان تفاعلات سكيرم تعتبر ملائمة مع نموذج القشرة لدراسة التركيب النووي.